

# Controlling the Population Imbalance of a Bose-Einstein Condensate by a Symmetry-Breaking Driving Field

Luis Morales-Molina<sup>1</sup> and Jiangbin Gong<sup>1,2</sup>

<sup>1</sup>*Department of Physics and Center for Computational Science and Engineering,  
National University of Singapore, 117542, Republic of Singapore*

<sup>2</sup>*NUS Graduate School for Integrative Sciences and Engineering, Singapore 117597, Republic of Singapore*

(Dated: October 25, 2018)

Nonlinear Floquet states associated with a symmetry-breaking driving field are exploited to control the dynamics of a Bose-Einstein condensate in a double-well potential. The population imbalance between the two wells is shown to be controllable by slowly tuning system parameters along a closed path. The results extend symmetry-breaking-based quantum control to many-body systems and extend navigation of linear Floquet states to navigation of nonlinear Floquet states.

PACS numbers: 32.80.Qk, 03.75.Nt, 05.45.-a, 03.75.Lm

Symmetry-breaking driving fields have found a variety of applications in quantum control, including the generation of photo-currents by harmonic mixing [1], the realization of basic mechanisms of ratchet transport [2], and the control of chiral processes [3], to name a few. To explore how symmetry-breaking driving fields can be used to manipulate the dynamics of Bose-Einstein condensates (BEC), it is necessary to extend symmetry-breaking-based quantum control scenarios to interacting many-body systems.

Given the robustness inherent in adiabatic quantum control, one wonders how a driven BEC system may be manipulated by slowly tuning the system parameters, especially those of the driving fields. To that end one also needs to extend the conventional Floquet states to mean-field nonlinear Floquet states [4, 5, 6, 7], a new concept for understanding periodically driven nonlinear systems. Nonlinear Floquet states may display degeneracy as well as bifurcation points that are absent in linear systems [6, 7]. This presents both challenges and opportunities for adiabatic quantum control. In particular, the number of nonlinear Floquet states can differ from the dimension of the Hilbert space, and that the adiabatic following of nonlinear systems might necessarily break down due to bifurcations [8].

In this study we demonstrate that the population imbalance of a BEC in a double-well potential [9, 10, 11, 12, 13] can be controlled (including its inversion) by using a symmetry-breaking driving field. Specifically, by considering a *closed* path of the system parameters, we show that it is possible to move one self-trapped state from one well to the other, thus inducing an inversion of the population imbalance and placing the system in a different nonlinear Floquet state. Recognizing that a double-well model is relevant to other contexts as well, e.g., a BEC occupying two hyperfine levels [14] or a BEC in an optical lattice that occupies two bands [15], this work shall motivate further studies of robust control of many-body quantum systems with symmetry-breaking driving fields.

A BEC in a double-well potential can be readily realized [11, 12, 13]. For example, the double-well po-

tential can be implemented by using two optical lattice potentials [16]. The periodic driving force can be created by modulating the relative phase between the two optical lattices [13] (see also [17]). Theoretically, under the mean-field two-mode treatment [18], the associated driven dynamics can be described as follows:

$$i\frac{d\psi_1}{dt} = C\psi_2 + g\psi_1N_1 + \psi_1f(t), \quad (1)$$

$$i\frac{d\psi_2}{dt} = C\psi_1 + g\psi_2N_2 - \psi_2f(t), \quad (2)$$

where  $C$  denotes the tunneling rate constant,  $g$  describes the nonlinearity due to the self-interaction of the BEC,  $N_{1,2} = |\psi_{1,2}|^2$  are the relative populations in the left or right wells (under the normalization  $N_1 + N_2 = 1$ ),

$$f(t) = f_1 \sin(\omega t) + f_2 \sin(2\omega t + \theta) \quad (3)$$

is a *zero-bias* bichromatic driving force with period  $T = 2\pi/\omega$ , and  $\theta$  is the relative phase between the  $\omega$  and  $2\omega$  fields. For a general value of  $\theta$  the bichromatic driving force  $f(t)$  breaks the time-reversal symmetry and a generalized parity [2]. Throughout we set  $\hbar = 1$ ,  $T = 1$  (hence all other parameters should be understood as scaled dimensionless variables). Typical values of these system parameters were well discussed in, e.g., Refs. [4, 19]. The value of  $g$  is assumed to be tunable via the Feshbach resonance under an external magnetic field, though the magnetic field is not explicitly included in the Hamiltonian.

For  $f(t) = 0$ , Eqs. (1) and (2) have a left-right permutation symmetry and reduce to the static double-well model for self-trapping [9, 10, 11]. That is, for a sufficiently large  $g$ , there exist two degenerate eigenstates with a nonzero population imbalance  $S \equiv N_1 - N_2$ . For  $f(t) \neq 0$ , in the linear limit the system (1)-(2) possesses two Floquet states whose time evolution satisfies  $[\psi_1(T), \psi_2(T)] = [\phi_1(0), \phi_2(0)] \exp(-i\epsilon)$ , where  $\phi_{1,2}(t+T) = \phi_{1,2}(t)$  and  $\epsilon$  is the quasienergy. The linear Floquet states can then be continuously extended into the nonlinear domain [7], thus defining nonlinear Floquet states. Like in the stationary case, Floquet states can also show

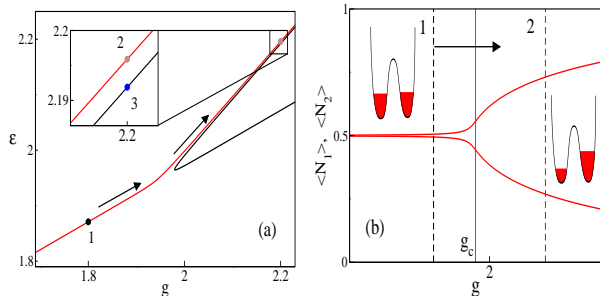


FIG. 1: (a) Quasienergy of nonlinear Floquet states vs the nonlinearity strength  $g$ . Points 1 and 2 represent the initial and final states in an adiabatic process (arrows indicate the direction). The population imbalance of state 3 on another branch is almost the opposite of that for state 2. (b) Populations for each well averaged over a driving period as  $g$  is adiabatically increased. The dashed lines labeled by 1 or 2 correspond to the states in (a). The thin solid line marks the threshold value  $g_c$  for the onset of self-trapping for  $\theta = -1.6$ . Insets depict the populations of atoms in the two wells for states 1 and 2. Other parameters are  $\omega = 2\pi$ ,  $f_1 = f_2 = 1$ ,  $C = 1$ .

population imbalance for large  $g$  as a manifestation of self-trapping.

To elucidate the properties of the nonlinear Floquet states we may also map the mean-field dynamics of the two-mode system onto the dynamics of a periodically driven classical system. Introducing the variable  $\varphi = \vartheta_2 - \vartheta_1$ , with  $\psi_1 = |\psi_1| \exp(i\vartheta_1)$  and  $\psi_2 = |\psi_2| \exp(i\vartheta_2)$ , a classical effective Hamiltonian  $H_{\text{eff}}$  exactly describing the dynamics of  $S$  and  $\varphi$  is found to be [5]  $H_{\text{eff}} = \frac{1}{2}gS^2 + C\sqrt{1-S^2}\cos(\varphi) + 2f(t)S$ . The nonlinear Floquet states can then be mapped to the fixed points of the Poincaré map of  $H_{\text{eff}}$  [4, 5].

To examine how the nonlinear Floquet states may be adiabatically correlated, we first study their behavior as the nonlinear parameter  $g$  increases. As we increases  $g$ , one of the two Floquet states can bifurcate into three nonlinear Floquet states at a critical value  $g_c$ . For the special cases of  $\theta = 0, \pi$ , the system conserves a generalized parity (time reversal together with a left-right permutation), we get a pitchfork bifurcation with two degenerate states with exactly opposite nonzero population imbalance  $S$ . When the above symmetry is broken a saddle node [Fig. 1] appears instead, where two of the new states have very close quasi-energies with almost opposite  $S$ ; and the third state corresponds to a saddle point on the Poincaré map of  $H_{\text{eff}}$ . In this latter case the critical nonlinearity value for the bifurcation is a function of  $\theta$ , denoted  $g_c(\theta)$ . The arrows in Fig. 1 show that with an adiabatic increase in  $g$  the system will continuously follow the upper bifurcation branch corresponding to a nonlinear Floquet state with increasing  $S$ .

Taking the parameter  $g$  as an example, how slowly the

system parameters should change in order to achieve necessary adiabaticity? To answer this question we consider cases of linear ramping, where  $g$  is made to change linearly in time, between  $g = g_1$  and  $g = g_2$ , at a rate of  $\alpha$ . To get a rough estimate of how small the ramping rate  $\alpha$  should be to ensure adiabaticity, we use the Landau-Zener tunneling formula of Floquet states in the linear limit [20]. For a representative case such as that shown in Fig.1, we find that  $\alpha \sim 10^{-4}$  suffices for an adiabatic process for which the Landau-Zener tunneling probability becomes negligible. To check that we take  $g_1 = 1.8$  and  $g_2 = 2.2$  and consider one initial state such as the state “1” shown in Fig. 1 (preparing such an initial state requires the tuning of  $S$  and  $\varphi$  [11], followed by a fast turn-on of the driving field). After the ramping we let the state evolve for some time and then examine the time dependence of  $N_1$  and  $N_2$ . For  $\alpha \leq 10^{-4}$ , the obtained state after the ramping process is essentially identical with the adiabatic state associated with  $g = g_2$  (or state “2” in Fig. 1). The periodic oscillations in  $N_1$  and  $N_2$  also exactly match the frequency of the driving field.

Significantly, if the main interest is in the control of the population imbalance  $S$ , then the averaged  $S$  over many cycles of the driving field is more relevant and hence it is unnecessary to achieve full adiabaticity. Consider then cases with considerably rapid ramping, e.g.,  $\alpha = 10^{-2}$  (so the ramping only need  $\sim 10^2$  field periods). As shown in Fig. 2, for such a ramping rate that is two orders of magnitude larger than before, almost the same time-averaged  $S$  is obtained. This can be further appreciated using an alternative perspective afforded by the classical effective Hamiltonian  $H_{\text{eff}}$ . As seen from the right panel in Fig. 2, if  $\alpha$  is much larger than  $10^{-2}$ , self-trapping breaks down. The classical trajectory after the ramping process is found to be on a chaotic layer around a separatrix structure, which corresponds to the state in the lowest bifurcation branch. This is understandable because after a fast ramping process, the system has not evolved much; so if the initial state is the fixed point for  $g = 1.8$  located at  $\varphi \approx -0.3$  and  $S \approx 0$ , it will necessarily find itself in the neighborhood of the saddle point for  $g = 2.2$  located also at  $\varphi \approx -0.3$  and  $S \approx 0$ .

By contrast, if  $\alpha \leq 10^{-2}$ , then the classical trajectory remains in the neighborhood of the fixed point. Averaging out the oscillations around the fixed point we obtain an averaged  $S$  close to that in the fully adiabatic case. Evidently then, manipulation of population imbalance may be effectively achieved within a relatively short time scale.

We now ask if the population imbalance  $S$  can be inverted. For that purpose the parameter  $\theta$  becomes crucial because it is responsible for the symmetry breaking here. However, for strong self-interaction  $g > g_c$ , a varying  $\theta$  may have little effect on a large  $S$  due to the self-trapping effect. Further, a path in the parameter space may not allow for adiabatic following if certain loop structure of nonlinear Floquet states is encountered (see, for example, case (c) of the lower panel of Fig. 4). This motivates

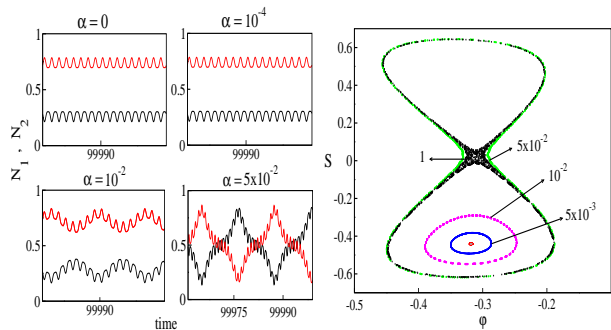


FIG. 2: Left panel: Evolution of the populations  $N_1$  and  $N_2$  after ramping the nonlinearity parameter  $g$  with different rates  $\alpha$ . Right panel: The same dynamics as in the left panel plotted on the  $S$ - $\varphi$  plane associated with  $H_{\text{eff}}$  in Eq. (4). Parameters are the same as in Fig. 1. The case of  $\alpha = 0$  represents the true adiabatic limit.

us to study how  $S$  might be inverted by tuning both  $\theta$  and  $g$ .

Consider then a four-stage control cycle with state 2 in Fig. 1 being the initial state. In stage I, the value of  $g$  is ramped from  $g = 2.2$  to  $g = 1.8$ , a point where degeneracy of nonlinear Floquet states no longer exists for any value of  $\theta$ . In stage II,  $\theta$  is ramped from  $-1.6$  to  $1.6$ . In stage III the value of  $g$  is ramped back to  $2.2$ , and in stage IV  $\theta$  is ramped back to  $-1.6$ . Stages III and IV are hence the opposite actions of stages I and II, but with a different order. As we ramp different parameters, we can have different ramping rates, e.g.,  $\alpha_g$ ,  $\alpha_\theta$ . For simplicity, we set the two ramping rates to be the same.

Figure 3 compares the time dependence of  $S$  associated with state 2 (bottom curve in the left panel) and that associated with the final state (upper curve with oscillations similar to state 2) after the four-stage ramping cycle, with the linear ramp rate in both  $g$  and  $\theta$  given by  $\alpha = 10^{-4}$ . Clearly, the resultant state after following the parameter cycle inverts  $S$ . Moreover, its dynamics coincides with that of state 3 (see Fig. 1). This indicates that after the four-stage control cycle, a nonlinear Floquet state different from the initial one is reached. Next we show in Fig. 3 the quasienergy along the control path. At first glance, the quasienergy path seems to form a closed loop. However, on a closer inspection of the last stage of the cycle (see panel (b) on the right of Fig. 3), it is found that the quasienergy of the final state (square) coincides with that of state 3 (see Fig. 1) and hence differs from that of the initial state (circle). This again confirms that the system is placed on a different nonlinear Floquet state after following the above ramping cycle.

To shed more light on the results we calculate the quasienergy surfaces as a function of  $\theta$  and  $g$  [Fig. 4]. For the sake of clarity, we only show the surface around the region where one quasienergy surface bifurcates into three surfaces. Above a critical strength of  $g$ , two quasi-

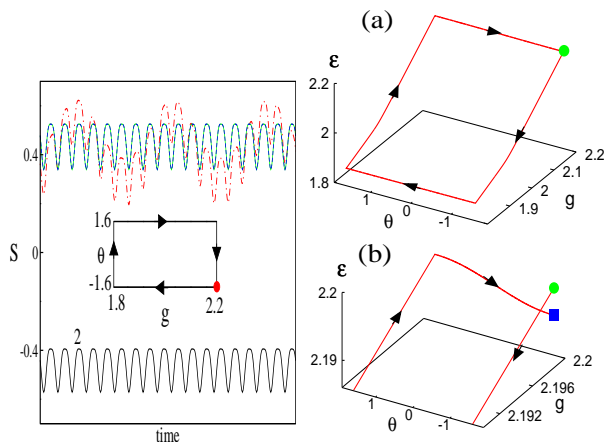


FIG. 3: Left panel: Population imbalance  $S$  of the initial state 2 (bottom curve) and the final state (upper curves) after a four-stage ramping cycle.  $\alpha = 10^{-4}$  for the upper solid curve and  $\alpha = 10^{-2}$  for the upper dotted-dashed curve. Inset: the four-stage cycle with the dot being the starting point. Right panel: (a) Quasienergy along the four-stage adiabatic cycle. (b) Enlargement of the panel (a). The initial and final points are depicted by a circle and square, respectively. Arrows indicate the direction of the ramping process.

energy surfaces can cross each other, forming a degeneracy line. Because this degeneracy line is along the  $\theta = 0$  direction (consistent with the fact that  $f(t)$  with  $\theta = 0$  conserves a generalized parity discussed above), the critical value  $g$  for the surface crossing can be identified as  $g_c(\theta = 0)$ . Note also that the degeneracy line does not present a problem for the system to continuously follow the ramping process, because (i)  $S$  can only change continuously and (ii) the involved degenerate states however have opposite values of  $S$ .

Using the quasi-energy surfaces and its projection at different  $g$  values, we can now visualize the dynamics associated with the above four-stage cycle. In the first stage, the state slides down the quasi-energy surface shown in Fig. 4, and at the same time three nonlinear Floquet states are merged into one. At the end of the first stage, the self-trapping phenomenon has disappeared and this makes it possible to reverse  $S$  by tuning  $\theta$ . The second step does exactly this by allowing the symmetry-breaking driving force to change  $S$  from a very small, negative value to a very small, but positive value. In the third stage, the  $g$  value returns to its original value, the system climbs up the quasi-energy surface, and three nonlinear Floquet states emerge again as a result of bifurcation. During this stage the inverted  $S$  is then magnified in the same mechanism as shown in Fig. 2. In the last stage when  $\theta$  is ramped back, the system can maintain its population imbalance due to self-trapping. In the meantime the system crosses the degeneracy line, returns all system parameters to their initial values, and finally ends up in a different Floquet state. This analysis also makes it clear that by considering a reversed closed path one

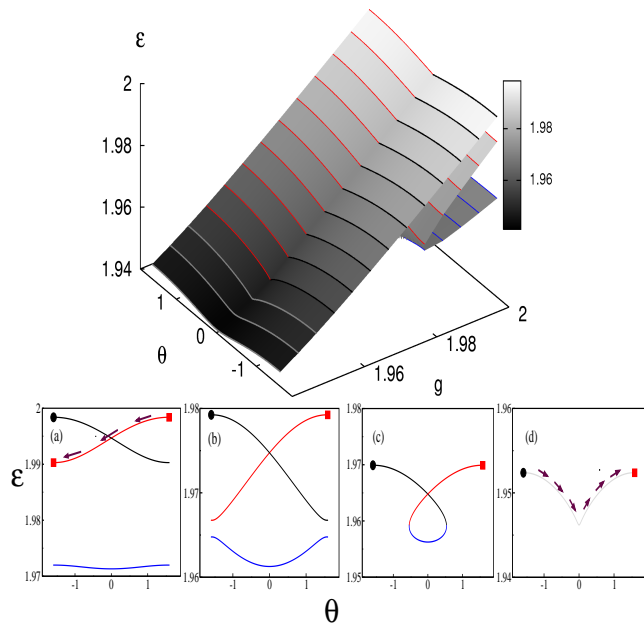


FIG. 4: Upper panel: Quasienergy surface vs the relative phase parameter  $\theta$  and the nonlinear parameter  $g$ . Lower panel: Quasienergy  $\epsilon$  vs  $\theta$  for various fixed values of  $g$ . (a)  $g = 2$ ; (b)  $g = 1.98$ ; (c)  $g = 1.97$ ; (d)  $g = 1.95$ . The initial state is depicted by a black dot in panel (a). In the first stage of the control cycle,  $g$  decreases and the quasienergy state (black dot) changes as shown in the a-b-c-d sequence of the four panels. Arrows in panel (d) indicates the evolution of the quasi-energy in the second stage. This yields a state with almost opposite population imbalance depicted by the square. In the third stage, in the order of d-c-b-a, the quasienergy (square) increases. The evolution in the final stage is indicated by the arrows in panel (a).

can also change  $S$  from positive to negative.

One may regard the above “anholonomy-like” behavior as a consequence of adiabatic following during the entire ramping process, insofar as the system always follows the control cycle and never populates two nonlinear Floquet states. However, due to the nonlinearity-induced degeneracy line along  $\theta = 0$ , it is better to regard the evolution during stage IV as a *diabatic* process. That is, during stage IV the change of the parameters is always “too fast” as compared with the zero spacing at the degeneracy point. Indeed, in a fully quantum treatment with-

out the mean-field approximation, the quantum levels, though nondegenerate, will be highly clustered around the mean-field degeneracy point. Therefore in a fully quantum picture adiabatic following breaks down during stage IV. In either perspective, the net result is the same: the system finds itself in a different state after following a ramping cycle in the parameter space.

We next examine whether we can achieve an inversion of  $S$  if the system parameters are tuned at a much faster rate? Significantly, as already suggested by the results in Fig. 2, the adiabatic following approach here still works even if we ramp the parameters  $g$  and  $\theta$  at a considerable rate. Indeed, the result for a ramping rate two orders of magnitude larger ( $\alpha = 10^{-2}$ ) is also shown in Fig. 3 (dotted-dashed curve on the left panel). In this case, as indicated by the beating patterns of the dynamics, the final state is not on one single Floquet state, but upon a time average we still achieve an inverted  $S$  close to that obtained from the previous slow ramping case. We have also checked many other clockwise (counter-clockwise) closed paths in the  $g - \theta$  plane of Fig. 4, finding that they can yield similar control from state 2 to state 3 (from state 3 to state 2) if they enclose the critical point  $g = g_c(\theta = 0)$ ;  $\theta = 0$ . Thus, we conclude that, given the topology of quasi-energy surfaces, especially the degeneracy and bifurcation points, navigation of nonlinear Floquet states provides a useful control scenario. This also extends an early control scenario based on the navigation of linear Floquet states [21]. Applying our approach to the cases with nonlinear Floquet states localized in momentum [7], it should be possible to invert ratchet transport in many-body systems without a biased field.

In conclusion, by demonstrating the control of the population imbalance associated with a BEC in a double-well potential, we have shown that the navigation of nonlinear Floquet states associated with symmetry-breaking driving fields can offer effective and robust control over many-body systems on the mean-field level.

**Acknowledgments:** We are grateful to Dr. Sergej Flach for interesting discussions and critical comments on early versions of this manuscript. One of the authors (J.G.) is supported by the start-up funding (WBS grant No. R-144-050-193-133/101) and the NUS “YIA” funding (WBS grant No. R-144-000-195-123). J.G. also thanks Zhang Qi for helpful discussions.

[1] G. Kurizki, M. Shapiro, and P. Brumer, Phys. Rev. B **39**, 3435 (1989); I. Goychuk and P. Hänggi, Europhys. Lett. **43**, 503 (1998).  
[2] S. Flach, O. Yevtushenko, and Y. Zolotaryuk, Phys. Rev. Lett. **84**, 2358 (2000); S. Kohler, J. Lehmann, and P. Hänggi, Phys. Rep. **406**, 379 (2005).  
[3] M. Shapiro and P. Brumer, Rep. Prog. Phys. **66**, 859 (2003).

[4] M. Holthaus, Phys. Rev. A **64**, 011601(R) (2001).  
[5] M. Holthaus and S. Stenholm, Eur. Phys. J. B **20** 451 (2001).  
[6] X. Luo, Q. Xie, and B. Wu, Phys. Rev. A **77** 053601 (2008).  
[7] L. Morales-Molina and S. Flach, New J. Phys. **10**, 013008 (2008).  
[8] B. Wu and Q. Niu, Phys. Rev. A **61**, 023402 (2000).

- [9] S. Aubry, S. Flach, K. Kladko, E. Olbrich, Phys. Rev. Lett. **76**, 1607 (1996).
- [10] A. Smerzi, S. Fantoni, S. Giovanazzi, and S.R. Shenoy, Phys. Rev. Lett. **79**, 4950 (1997).
- [11] M. Albiez *et al.*, Phys. Rev. Lett. **95**, 010402 (2005).
- [12] Y. Shin *et al.*, Phys. Rev. Lett. **92**, 050405 (2004).
- [13] E. Kierig, U. Schnorrberger, A. Schietinger, J. Tomkovic, M. K. Oberthaler, Phys. Rev. Lett. **100**, 190405 (2008).
- [14] M. R. Matthews *et al.*, Phys. Rev. Lett. **83**, 3358 (1999).
- [15] M. Jona-Lasinio *et al.*, Phys. Rev. Lett. **91**, 230406 (2003).
- [16] S. Fölling *et al.*, Nature **448**, 1029 (2007).
- [17] T. Salger, C. Geckeler, S. Kling, and M. Weitz, Phys. Rev. Lett. **99**, 190405 (2007).
- [18] G.J. Milburn, J. Corney, E. M. Wright, D. F Walls, Phys. Rev. A **55**, 4318 (1997).
- [19] C. Weiss and T. Jinasundera, Phys. Rev. A **72**, 053626 (2005).
- [20] H. P. Breuer and M. Holthaus, Z. Phys. D **11**, 1 (1989).
- [21] L. Morales-Molina, S. Flach, and J.B. Gong, Europhys. Lett. (in press). See also arXiv:0805.0827.